NASA TECHNICAL MEMORANDUM

NASA TM X-67991

NASA TM X-67991

EXTERNALLY-BLOWN-FLAP NOISE

by Robert G. Dorsch, Walter J. Kreim, and William A. Olsen
Lewis Research Center
Cleveland, Ohio

TECHNICAL PAPER proposed for presentation at
Tenth Aerospace Sciences Meeting sponsored by
the American Institute of Aeronautics and Astronautics
San Diego, California, January 17-19, 1972

EXTERNALLY-BLOWN-FLAP NOISE

by Robert G. Dorsch, Walter J. Kreim, and William A. Olsen
Lewis Research Center
National Aeronautics and Space Administration
Cleveland, Ohio

Abstract

Noise data were obtained with a large externally blown flap model. A fan-jet engine exhaust was simulated by a 1/2-scale bypass nozzle supplied by pressurized air. The nozzle was pylon mounted on a wing section having a double-slotted flap for lift augmentation. Noise radiation patterns and spectra were obtained for nozzle exhaust velocities between 400 and 1150 ft/sec. The blown flap noise data are in good agreement with previous small model results extrapolated to test conditions by Strouhal scaling. The results indicate that blown flap noise must be suppressed to meet STOL aircraft noise goals.

Introduction

The externally blown flap (EBF) is one of the primary contenders as a lift augmentation device for STOL aircraft (fig. 1). In view of the stringent noise restriction goals (95 EPNdB at 500 ft) which have been set for the development of STOL aircraft, it is important to measure and carefully evaluate the noise generated and redirected by these devices. Previous EBF noise tests have been made with very small models.[1-4] These data have been extrapolated up to full scale airplane flap systems in order to obtain EBF noise estimates (e.g., refs. 2 and 3). The estimates have indicated that for an EBF STOL airplane equipped with quiet engines the blown flap noise will be the major contribution to the total aircraft noise at all except the very lowest blowing velocities. In view of the large extrapolations required in these estimates large scale EBF noise data are needed to check the predictions and to establish the validity of the scaling laws employed.

Noise tests were therefore conducted at the Lewis Research Center with a large externally blown flap model. The exhaust of a 10 000 lbf thrust fan-jet engine with a bypass ratio of six was simulated by a 1/2-scale model of its bypass nozzle supplied by pressurized air. The nozzle assembly was pylon mounted on a 1/2-scale-chord wing section having a large double-slotted flap for lift augmentation. Tests were also run with the bypass nozzle replaced by a single convergent nozzle having a 13 inch diameter in order to facilitate comparison with the earlier small scale data of references 3 and 4.

The EBF noise data obtained in the large-scale tests are summarized in this paper. The results are compared with the earlier small scale data and the validity of the scaling laws is established. The flap noise data for the 1/2-scale model are extrapolated to a similar full-scale blown flap system for a 4-engine plane in the 70 000 lb class and the noise level is assessed.

Apparatus and Procedure

Model Configuration

The externally blown flap configuration shown in figures 2 and 3 is based on one of the double slotted external flow jet flap configurations developed by the NASA Langley Research Center.[5,6] The wing section (fig. 2) had a chord length of 82 inches (flaps retracted) and a span of 9 feet. The flaps could be set at 30°-60°, 10°-20°, and 0° (retracted) positions. The 30°-60° flap angle notation, for example, means that the leading flap is lowered 30° and the trailing flap 60° from the wing reference chord line. The flaps were blown by an air jet exhausting from a bypass nozzle pylon-mounted on the wing as shown in figure 2(a) and 3(a). The core nozzle was circular with an 8.15 inch diameter and the bypass nozzle (fan exhaust) was annular with an inner diameter of 18 inches and an outer diameter of 23.25 inches. The annulus height was 2.63 inches. The annular nozzle was located 15 inches ahead of the wing leading edge and core exhaust plane was 7 inches downstream of the leading edge. In order to direct the exhaust toward the flaps the nozzle axis was at a 5° angle with respect to the reference chord line of the wing as shown in figure 2(a). Noise tests were also run with the pylon-mounted bypass nozzle replaced by a 13-inch diameter circular convergent nozzle located 15 inches ahead of the wing leading edge (fan exhaust plane) as shown in figures 2(b) and 3(b).

The EBF model was mounted with the wing in a vertical position with the axis of the nozzle 12'9-3/4" above grade. The nozzle axis was located at a spanwise position 5 feet from the bottom of the wing section and 4 feet from the top to minimize support structure interference with spanwise flow on the flaps.

Noise tests were also run with each nozzle with the wing removed so that the nozzle-alone noise could be measured.

Air Flow System

The exhaust nozzles were supplied with ambient dry air from the Center's propulsion air supply system (150 psig max.) brought to the test site by a 24 inch diameter underground line. An orifice flowmeter was located in a straight section of the underground line upstream of the 16 inch gate shutoff valve at the test site. The EBF test rig flow system was connected to the gate valve and is shown in figure 4.

The operating pressure ratio (nozzle total pressure divided by the ambient atmospheric pressure) for the bypass nozzle core and the 13 inch convergent nozzle was set by the flow control valve and supply pressure. A pressure drop screen in the annulus of the bypass nozzle assembly determined the corresponding pressure ratio for the simulated fan exhaust. The screen provided a nominal ratio of fan exhaust velocity to core exhaust velocity of 0.78. This ratio varied from 0.68 at a core PR of 1.1 to 0.85 at a PR of 2.2.

Nozzle total pressures and temperatures were

TM X-67931

measured at the nozzle inlets (downstream of the screen in the case of the annular nozzle). The nozzle exhaust velocities were determined from the isentropic equations.

Two flow distribution and quieting screens were located (fig. 4) between the last elbow of the flow system and the nozzle assemblies.

Internal Noise Suppression

The unsuppressed internal flow noise for this system had a sound power level greater than 153 dB at all operating conditions. In order to measure jet noise at the lower pressure ratios of this test it was necessary to remove 25 to 30 dB of this noise with a muffler system.

The muffler system (fig. 4) consisted of overlapping low, middle, and high frequency attenuators. Low frequency quieting was obtained by using perforated plates as pressure drop devices just downstream of the flow control valve (the principal noise source) and at the exit of the middle frequency muffler. These plates have a low admittance to low frequency noise and also serve as flow redistributors.

The middle frequency muffler consisted of a 3 foot diameter 6 foot long pipe with crossed splitter plates to divide the flow into four channels. All inside surfaces were lined with one inch thick hair felt held in place by expanded metal (70% open). The perforated plate at the end of this section had 1/8 inch diameter holes and was 20 percent open.

The high frequency muffler section was located at the downstream end of the upper (and last) elbow of the flow system to take advantage of multiple reflections associated with the flow turn. A crossed splitter plate divided the flow into four channels. All pipe walls and both sides of the horizontal splitter plate were lined with one inch thick plastic felt material held in place by expanded metal (70% open). The first of the final two flow distribution and quieting screens was located immediately downstream of this muffler.

Finally, to prevent direct radiation of internal noise transmitted through the pipe walls the flow system was wrapped with a 2 inch thick layer of fiberglass covered by leaded-vinyl plastic sheet material.

Acoustic Instrumentation and Analysis

The noise data were measured with 20 1/2-inch condenser microphones located 12'9-3/4" above a hard surface (black top). The microphones were placed on a 50 foot radius circle in a horizontal plane perpendicular to the vertically mounted wing. The center of the microphone circle was located on the nozzle axis centerline halfway between the core nozzle exhaust plane and the point of intersection with the 60° flap (fig. 2(a)).

The noise data were analyzed on-line with an automated 1/3-octave band spectrum analyzer. The analyzer determined sound pressure level spectra (referenced to 0.0002 microbar) between 50 and 20 000 Hz at each microphone position. A four second integration time was used. Three noise samples were taken at each microphone and treated statistically to reject background disturbances and random errors and to obtain either an average or most probable value. The data were then corrected for atmospheric attenuation to give lossless data at 50 feet. From these sound pressure level spectra the overall sound pressure levels and perceived noise levels were calculated at each microphone location.

The combination of microphone height and distance from the model was selected (after a trial run in which they were varied) to give acceptable cancellation and reinforcement amplitudes caused by ground reflections. The ground reflections were estimated to increase the overall sound pressure level (OASPL) by only 1.5 to 2 dB at the selected microphone locations. The data of this report therefore generally do not include ground reflection corrections except when making spectral comparisons. In these cases (noted in the paper) corrections to the SPL at each frequency were made by an adaptation of the method of reference 7 which is an extension of Howe's model.(8)

Test Procedure

For each model configuration tested noise measurements were made for a series of nominal nozzle pressure ratios. These were 1.1, 1.2, 1.3, 1.4, 1.5, 1.7, 1.8, 2.0, and either 2.1 or 2.2.

The nozzle stagnation temperature varied between 55° and 82° F for the test series.

The exhaust velocities for each nominal pressure ratio setting were calculated from the measured values of nozzle pressure ratio and stagnation temperature. These velocities were used in the analysis of the acoustic data.

The exhaust flow of both nozzles was also surveyed with a total pressure rake in order to obtain velocity profiles at various axial locations along the nozzle centerline.

Exhaust-Jet Velocity Profiles and Boundaries

The radial velocity profiles for the 13 inch convergent nozzle exhaust (wing removed) are shown in figure 5 for two axial locations downstream of the exit plane. The velocity profiles at 13 inches ($X/D = 1.0$) are shown for several pressure ratios in figure 5(a). At this station the flow is typical of potential core flow with very little evidence of mixing. At 94 inches from the nozzle ($X/D = 7.2$) which is the distance along the centerline to the impingement point on the 60° flap (fig. 2(b)) the jet has become thoroughly mixed and the peak velocity at each pressure ratio has decayed to about 0.94 of the nozzle exit value.

Radial velocity profiles for the bypass nozzle exhaust flow (wing and pylon removed) are shown in figure 6. Figure 6(a) shows that 8 inches downstream of the core nozzle exit ($X/D_c = 1.0$) the potential core region of the annular (fan) nozzle exhaust flow has already mixed out because of its small height and upstream location. At 72 inches (centerline impingement point on 60° flap) it can be seen in figure 6(b) that the annular nozzle flow can no longer be distinguished and the core nozzle flow has become well mixed. At this location ($X/D_c = 9.0$) the peak velocity at most pres-

sure ratios is nearly the same as the nozzle exhaust velocity. That is, the decay of the core jet has been delayed by the presence of the surrounding annular exhaust flow.

Approximate exhaust jet boundaries (V = 0) and their location with respect to the wing and flap system are shown in figure 7. For both nozzles the amount of scrubbing by the exhaust on the wing proper (upstream of the flaps) was small.

Scaling Method

Blown flap noise estimates were made for a full size STOL airplane. The perceived noise level (PNL) at 500 feet in a given direction was calculated from the measured SPL spectral data as follows. First all model nozzle, nozzle location, and wing and flap dimensions were linearly scaled up to conform to the full scale nozzle exhaust area required at each pressure ratio in order to obtain the specified engine thrust. The noise data measured at a given pressure ratio and microphone was then extrapolated by assuming that the frequency of the 1/3-octave spectrum could be scaled by using the Strouhal reciprocal relationship between frequency and nozzle diameter. The magnitude at each frequency was assumed to be proportional to the nozzle area, the number of engines, and the inverse square of the distance. The resultant 1/3-octave SPL spectrum was then corrected for atmospheric absorption and the PNL was then calculated in the usual manner.

Results and Discussion

The sound data obtained with the 1/2-scale model EBF having the pylon mounted bypass nozzle (figs. 2(a) and 3(a)) will be summarized first. These results will be followed by a comparison of the EBF data obtained using the 13 inch convergent nozzle with earlier small-scale results for the identical configuration.

Bypass Nozzle EBF

Noise radiation patterns. The blown flap noise radiation pattern at a 50 foot radius is shown in polar form in figure 8 for a core nozzle pressure ratio of 1.4. The core exhaust velocity was 765 ft/sec and the annular nozzle (fan) exhaust velocity was 582 ft/sec. The overall sound pressure level (OASPL) as a function of microphone angle, θ, is given for flap positions of 30°-60°, 10°-20°, and 0° (fully retracted) and for the nozzle alone. As has been noted with the previous small model results[3] there is a large increase in noise below the wing as the flaps are lowered into the nozzle exhaust. For example at $\theta = 90^\circ$ (which would be directly below the airplane) there is a 10 dB increase in noise when the flaps are lowered from the retracted (0°) to the 30°-60° flap position. Note also that the noise for the bypass nozzle installed below the wing (0° flap data) is considerably louder at most angles than the noise for the bypass nozzle alone.

The noise radiation patterns at 50 feet for the four test configurations are summarized in figure 9 for selected core nozzle pressure ratios between 1.1 and 2.1. The patterns for the bypass nozzle alone (but including pylon) are given in figure 9(a). The presence of the attached pylon assembly introduces some nonsymmetry (about $\theta = 180^\circ$) to the nozzle noise radiation patterns. The data for the blown flaps at positions of 0° (retracted), 10°-20°, and 30°-60° are given in 9(b), 9(c), and 9(d), respectively. These figures show that the noise increases with flap deflection angle at all pressure ratios, and for a given flap setting the noise increases strongly with exhaust velocity. At high flap angle settings (30°-60°) the flap interaction (or impingement) noise completely dominates the sound field so that the radiation patterns of figure 9(d) show little change in shape with pressure ratio. At low flap angles the nozzle exhaust jet noise makes a significant contribution to the total noise at the higher exhaust velocities causing some change in shape of the 0° and 10°-20° patterns as the core nozzle pressure ratio increases.

Sound pressure level spectra. In order to determine the perceived noise level below an EBF aircraft it is necessary to know the SPL spectra of the blown flap as a function of angle. Typical 1/3-octave SPL spectra measured at 50 feet directly below the wing model ($\theta = 85^\circ$) for the four test configurations are given in figure 10 for pressure ratios of 1.4 and 1.7. The spectra are broad band and have been corrected for ground effects. The strong increase in sound pressure level as the flaps are lowered into the jet exhaust is again readily apparent. Further the SPL curve peaks at higher frequencies as the flaps are lowered.

To assist in evaluating the perceived noise level at sideline stations a limited amount of data were also taken with an overhead microphone suspended 50 feet above the vertically mounted wing model (in the wing-tip direction). The 1/3-octave SPL spectra for the 30°-60° flap configuration measured with the overhead microphone are shown in figure 11 for core nozzle pressure ratios between 1.2 and 2.1. These data were not corrected for ground effects because with the microphone in the overhead position the reflected rays are scattered as they pass through the jet exhaust. The sideline SPL values at each pressure ratio are as much as 10 dB lower than the corresponding 30°-60° data of figure 10. There is also a change in spectrum shape. The corresponding OASPL values at each pressure ratio are also given in figure 11 along with the decrease (Δ dB) from the $\theta = 85^\circ$ value of figure 9(d).

Perceived noise level. The perceived noise level (PNL) was calculated from the 1/3-octave SPL spectral data. The radiation patterns obtained at 500 feet distance from the 1/2-scale model for two flap deflections are given in figure 12 for core nozzle pressure ratios between 1.1 and 1.7. The 10°-20° flap results are given in figure 12(a) and the 30°-60° results are given in figure 12(b). Figure 12 shows that the 95 PNdB level is exceeded for the 10°-20° flap setting at a core nozzle pressure ratio of 1.7 and at pressure ratios above 1.3 for the 30°-60° case. It is clear that a noise problem exists for this EBF system.

The PNL at 500 feet from the 1/2-scale model for the four test configurations are given as a function of the nozzle core exhaust velocity in figure 13. The PNL values directly below the wing ($\theta = 85^\circ$) are given for each configuration in fig-

ure 13(a). The values given in figure 13(b) for each configuration are for the direction which produces a maximum in PNL during a flyover. Figure 13 shows the same strong effect of both exhaust velocity and flap deflection angle on PNL as was observed in the OASPL data. For example figure 13(b) shows that the PNL increases about 4 PNdB when the flaps are lowered from the retracted (0^o) to the 10^o-20^o position. Lowering the flaps further (from 10^o-20^o to 30^o-60^o) causes 8 PNdB in additional noise.

Comparison with Small Scale EBF Data

The 1/2-scale model blown by the 13 inch diameter circular convergent nozzle is geometrically identical to the small (1/13) scale EBF model used in previously reported tests at the Lewis Research Center.[3,4] The 1/13 scale model had a 2 inch diameter circular convergent nozzle and a wing chord of 12.6 inches (fully retracted). The data were taken at a microphone radius of 10 feet.

The noise radiation patterns for the two models with 30^o-60^o flap settings are compared in figure 14 for nozzle pressure ratios of 1.4, 1.7, and 2.2. The small scale model OASPL data have been scaled up to the 1/2-scale results at 50 foot radius by adding

$$10 \log\left[\left(\frac{D_{1/2}}{D_{1/13}}\right)^2 \times \left(\frac{R_{1/13}}{R_{1/2}}\right)^2\right] = 10 \log\left[\left(\frac{13}{2}\right)^2 \times \left(\frac{10}{50}\right)^2\right]$$

which is 2.3 dB to the small scale values. The comparison shows that nearly identical OASPL radiation patterns were obtained with the two different size models.

In order to compare 1/3-octave spectral data results it is necessary to use the Strouhal relation between frequency, nozzle diameter (D), and exhaust velocity (V) in order to scale frequency in addition to the magnitude of the sound pressure level. The validity of using Strouhal scaling was established as follows. The 1/3-octave SPL data obtained at the $\theta = 85^o$ microphone with the two models (flaps at 30^o-60^o) were first corrected for ground effects and then converted to Normalized SPL Spectral Density (SPL - OASPL + 10 log V/D - 10 log Δf) and plotted versus the Strouhal Number (f D/V) as shown in figure 15. The data points shown in figure 15 are for the 1/2-scale model with nozzle exhaust velocities between 571 and 1128 ft/sec. The curve shown was obtained from a fit to a similar set of 1/13-scale-model data points. Figure 15 shows that the Strouhal relation correlates the 1/2-scale model data very well over the velocity range. The results indicate that the exhaust velocity which is proportional to flap impingement velocity can be used for scaling frequency. Further there is very good agreement between the large and the small scale data. Thus the model linear scale factor (proportional to nozzle diameter ratio) can also be used to scale frequency. The only significant difference between the large and small model results shown in figure 15 is in the high frequency slope. The large model values decrease at a somewhat slower rate with frequency. However, the values differ significantly only above a Strouhal number of 1.5 at which the magnitudes are down 15 dB from the peak value. Although one might suspect residual unsuppressed internal noise in the 1/2-scale data as the cause of the difference in slope, close examination of the trends with velocity does not bear out this hypothesis. The differences are not fully understood at this time.

If velocity is held constant scaling is simplified. The small scale 1/3-octave spectra can be scaled to the 1/2-scale data by adding 2.3 dB to the SPL magnitudes and dividing the 1/3-octave frequencies by the 6.5 scale factor (diameter ratio). Figure 16 shows such a comparison obtained for a pressure ratio 1.7 run with the flaps at 30^o-60^o. The data were corrected for ground effects to facilitate comparison. Again the agreement is found to be excellent.

The results of figures 14 through 16 show that there is very good agreement between the data of this study and the previous small scale results. Further, the results indicate that the 1/2-scale model data can be scaled to a value representing a full size EBF system by the same technique.

Extrapolation to Full Scale EBF System

Blown flap noise estimates were made for a hypothetical 4-engine 70 000 lb gross weight STOL aircraft having a total thrust of 40 000 lbf. The maximum perceived noise level which would occur during a 500 foot flyover was calculated for both the takeoff and landing conditions. The takeoff condition was assumed to be 100 percent thrust (10 K per engine), 10^o-20^o flap angle setting, and a climb angle of 15^o with respect to the horizontal (ground) plane. The landing condition was assumed to be 60 percent thrust, 30^o-60^o flap angle, and an approach angle of -7.5^o with respect to horizontal. The 500 foot maximum sideline PNL was also estimated for each condition. No adjustments for relative velocity effects on the blown flap noise were included in the estimates because data on the effect of airplane forward velocity on blown flap noise was not available to the authors. However, the effect of forward velocity on the flap interaction (or scrubbing) noise is expected to be small. It is further assumed in the estimates that the rotating machinery noise (fan and turbine) has been suppressed leaving the jet exhaust mixing and flap interaction as the dominant noise sources.

The full scale airplane blown flap noise estimates based on the data from the 1/2-scale model are summarized in figure 17 for the assumed takeoff and landing conditions. The perceived noise levels given in figure 17 are as much as 21 dB above the 95 PNdB goal. Thus the results of this test indicate that a very large amount of flap noise suppression would be required for flaps blown by fan jet engines having exhaust velocities in this range.

The test data along with the results of previous studies indicate that a larger diameter engine having lower exhaust velocities would reduce the blown flap noise. An estimate of the effect of exhaust velocity on the blown flap noise for the hypothetical 70 000 lb STOL aircraft is shown in figure 18. These estimates assume that the engines have a ratio of fan exhaust velocity to core exhaust velocity near unity (instead of 0.78) and are therefore based on the 13 inch con-

vergent nozzle EBF data. The upper limit of the scatter bands shown is based on the previously described scaling assumption that the flap dimensions (and all others) increase linearly with the engine diameter. This assumption leads to overly large wing and flap chord lengths for a 70 000 lb aircraft at the lower exhaust velocities. The lower limit of the scatter band was obtained by holding the flap dimensions constant at full size (twice the model size). This assumption results in reduced lift augmentation at large engine diameters. The 500 foot perceived noise level estimates for both the takeoff and landing condition are given in figure 18. The corresponding fan exhaust nozzle pressure ratio at takeoff is also indicated. The takeoff PNL during a 500 foot flyover at a fan nozzle pressure ratio of 1.3 (693 ft/sec) is estimated to be between 100 and 102.5 PNdB. At the corresponding landing condition (475 ft/sec) the PNL is estimated to be between 96 and 98.5 PNdB.

The estimates given in figure 18 indicate that substantial blown flap noise reduction can be achieved by going to high-bypass low-pressure-ratio engines having low exhaust velocities. It appears possible with an airplane of this size to reduce the blown flap noise to below 95 PNdB by using an engine with takeoff exhaust velocities below 600 ft/sec. At higher exhaust velocities some form of blown flap noise suppression appears to be required.

A possible method of suppressing the blown flap interaction noise is to use a mixer nozzle at the engine exhaust exit to reduce the velocity of impingement on the flaps.[9-11] A photograph of a research mixer nozzle is shown on the 1/2-scale EBF test rig in figure 19. Preliminary measurements with the flaps in the 30^{o}-60^{o} position indicate that about 5 PNdB flap noise suppression can be obtained at 500 feet below the airplane at the landing attitude by employing an exhaust nozzle of this type. However, the preliminary data also indicate that the mixer nozzle was ineffective as a flap noise suppressor when the flaps were at the 10^{o}-20^{o} position. Further research is being conducted to establish the noise suppression potential of this concept.

Concluding Remarks

The agreement between the blown flap noise measured at a given nozzle exhaust velocity with the 1/2-scale model of this study and the values predicted from earlier data measured at the same velocity with a 1/13-scale model of the identical EBF configuration was excellent. These results give confidence that noise data from linearly scaled EBF models can be used to predict full size airplane blown flap noise. Implicit in this type of scaling of an EBF system is that the model exhaust nozzle is located at the same number of diameters from the flap system so that the peak velocity decay and the velocity profile at the flaps are the same as for the full size system. Thus the location and area of the scrubbing zone and the scrubbing velocity distribution in this zone will be properly scaled along with the flap geometry.

The STOL airplane blown flap noise estimates of this paper were made for an airplane having an EBF system geometry identical to the test model. The linear scale factor at each exhaust velocity was dictated by the particular thrust level chosen. At the present state of the art it is not possible to make predictions (or even to accurately compare data) for an EBF system having significantly different geometry and/or exhaust velocity profiles at the flaps. The effects of differences in exhaust velocity profiles and decay rates, in wing and flap geometry, and in nozzle shape, location, and orientation are not well enough known at present. Further research studies are required in these areas along with research on methods of suppressing blown flap noise.

References

1. Maglieri, D. J. and Hubbard, H. H., "Preliminary Measurements of the Noise Characteristics of Some Jet-Augmented-Flap Configurations," Memo 12-4-58L, 1959 NASA, Hampton, Va.

2. Kramer, J. J., Chestnutt, D., Krejsa, E. A., Lucas, J. G., and Rice, E. J., "Noise Reduction," Aircraft Propulsion, SP-259, 1971, NASA, Washington, D.C., pp. 169-209.

3. Dorsch, R. G., Krejsa, E. A., and Olsen, W. A., "Blown Flap Noise Research," AIAA paper 71-745, June 1971.

4. Olsen, W. A., Dorsch, R. G., and Miles, J. H., "Noise Produced by a Small-Scale Externally Blown Flap," TN D-6636, 1972, NASA, Cleveland, Oh.

5. Parlett, L. P., Freeman, D. C., Jr., and Smith, C. C., Jr., "Wind-Tunnel Investigation of a Jet Transport Airplane Configuration With High Thrust-Weight Ratio and an External-Flow Jet Flap, NASA TN D-6058, 1970, NASA, Hampton, Va.

6. Freeman, D. C., Jr., Parlett, L. P., and Henderson, R. L., "Wind-Tunnel Investigation of a Jet Transport Airplane Configuration With an External-Flow Jet Flap and Inboard Pod-Mounted Engines," NASA TN D-7004, 1970, NASA, Hampton, Va.

7. Thomas, P., "Etude des Interferences Acoustiques par Reflexion. Application aux Spectres de Pression Acoustique des Jets," Aircraft Engine Noise and Sonic Boom, AGARD CP No. 42, May 1969, Saint Louis, France.

8. Howes, W. L., "Ground Reflection of Jet Noise," TR-35, 1959, NASA, Washington, D.C.

9. Goodykoontz, J. H., Olsen, W. A., and Dorsch, R. G., "Preliminary Tests of the Mixer Nozzle Concept for Reducing Blown Flap Noise," TM X-67938, 1971, NASA, Cleveland, Oh.

10. Groesbeck, D., Huff, R., and von Glahn, U., "Peak Axial-Velocity Decay With Mixer-Type Exhaust Nozzles," TM X-67934, 1971, NASA, Cleveland, Oh.

11. von Glahn, U. H., Groesbeck, D. E., and Huff, R. G., "Peak Axial-Velocity Decay With Single- and Multi-Element Nozzles," To be presented at this conference.

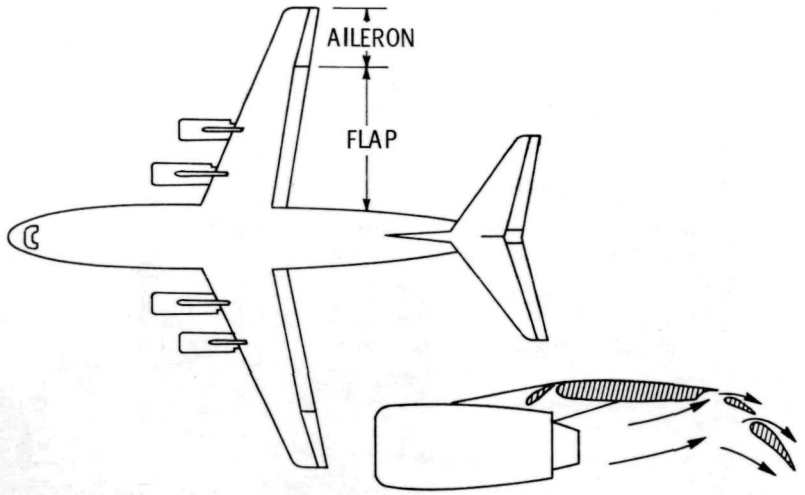

Figure 1. - Externally-blown-flap STOL airplane.

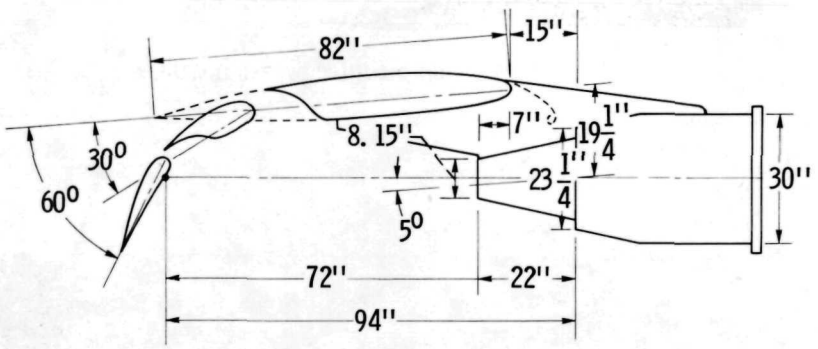

(a) With pylon mounted bypass nozzle.

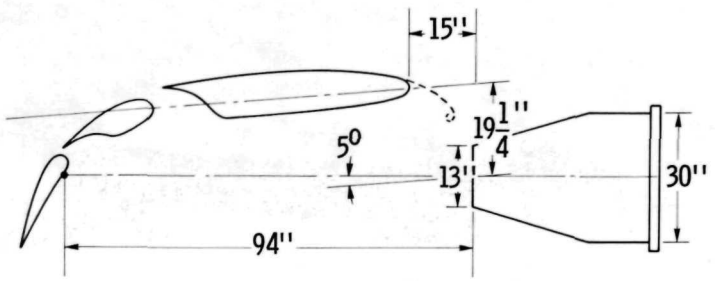

(b) With 13-inch-diameter convergent nozzle.

Figure 2. - Test configurations for 1/2-scale externally blown flap model.

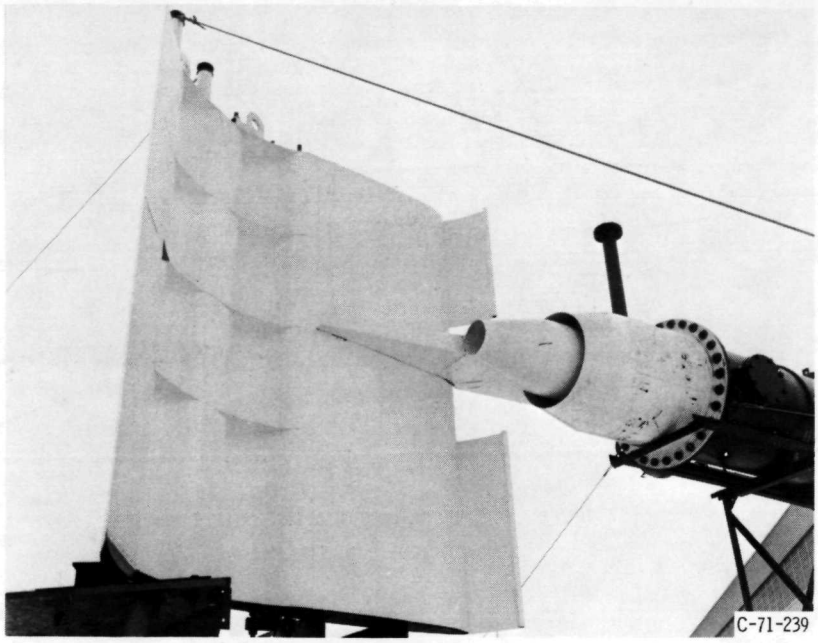

(a) With pylon mounted bypass nozzle.

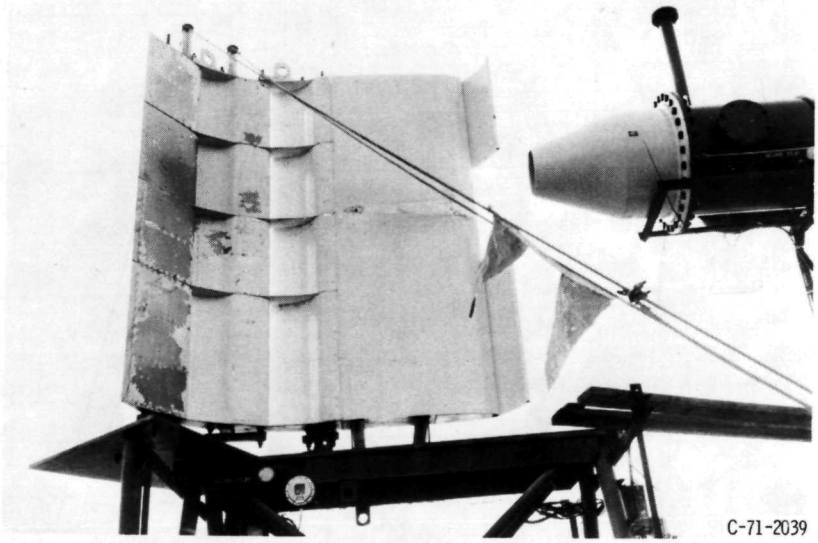

(b) With 13 inch diameter nozzle.

Figure 3. - Externally-blown-flap model.

E-6737

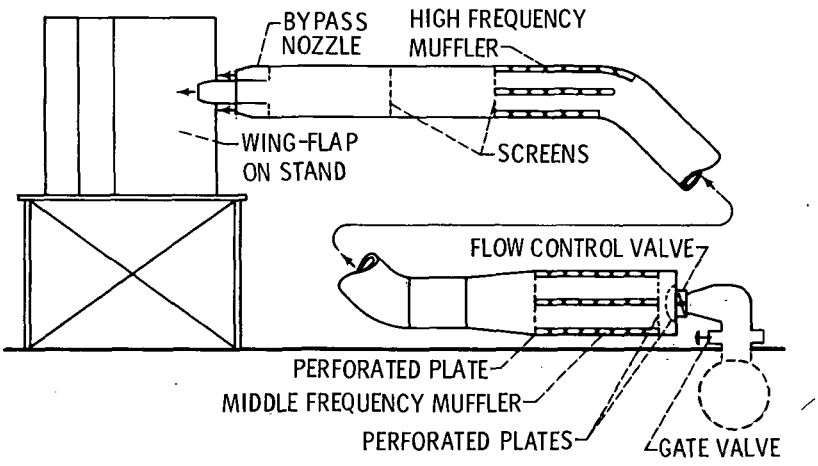

Figure 4. - Nozzle air supply system.

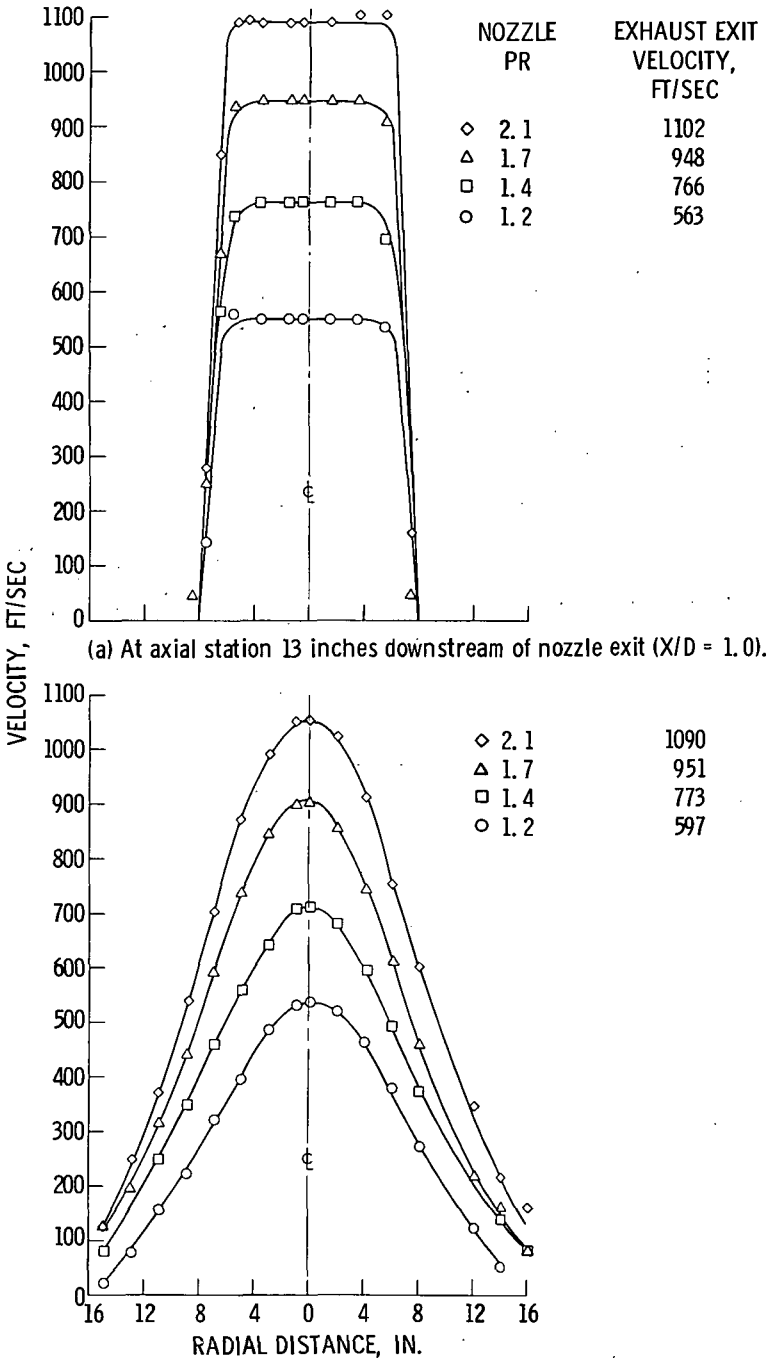

(a) At axial station 13 inches downstream of nozzle exit (X/D = 1.0).

(b) At axial station 94 inches downstream of nozzle exit (X/D = 7.2).

Figure 5. - Thirteen-inch round convergent nozzle exhaust velocity profiles.

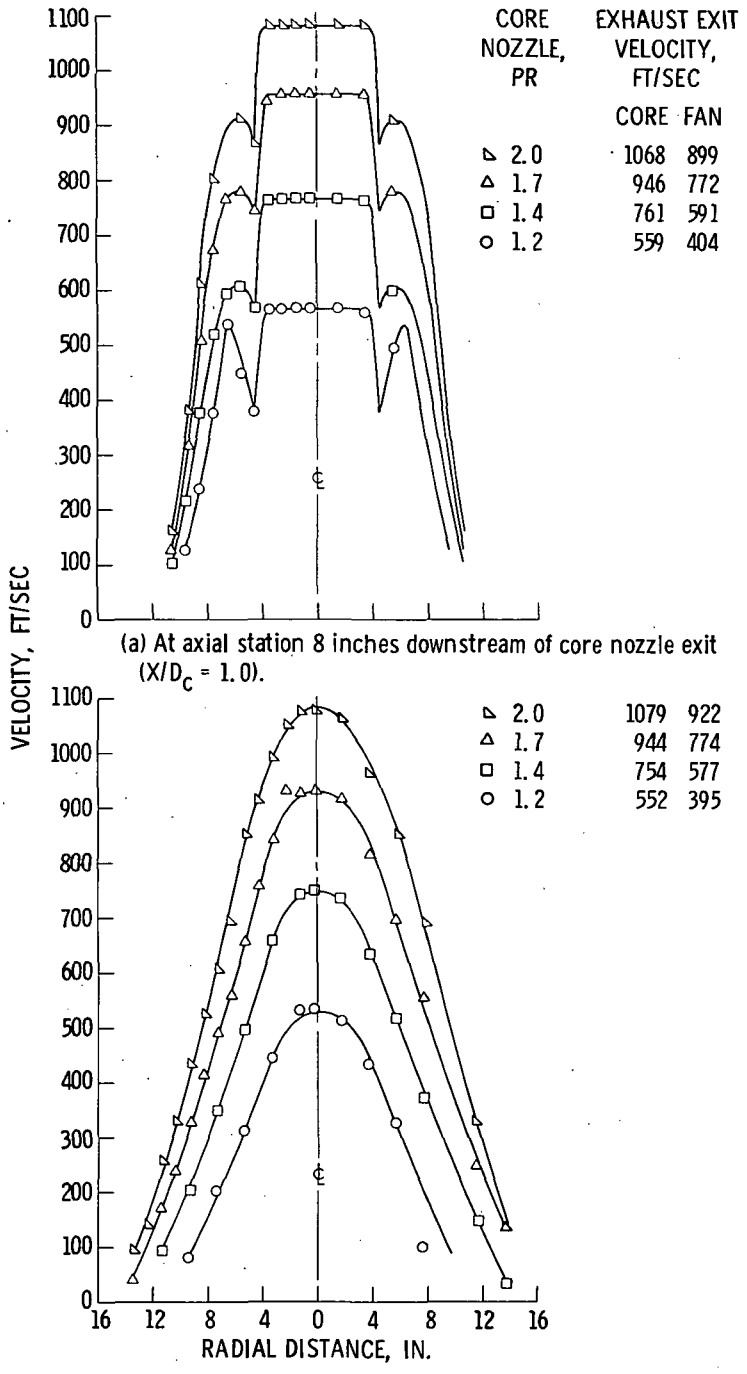

(a) At axial station 8 inches downstream of core nozzle exit ($X/D_c = 1.0$).

(b) At axial station 72 inches downstream of core nozzle exit ($X/D_c = 9.0$).

Figure 6. - Bypass nozzle exhaust velocity profiles.

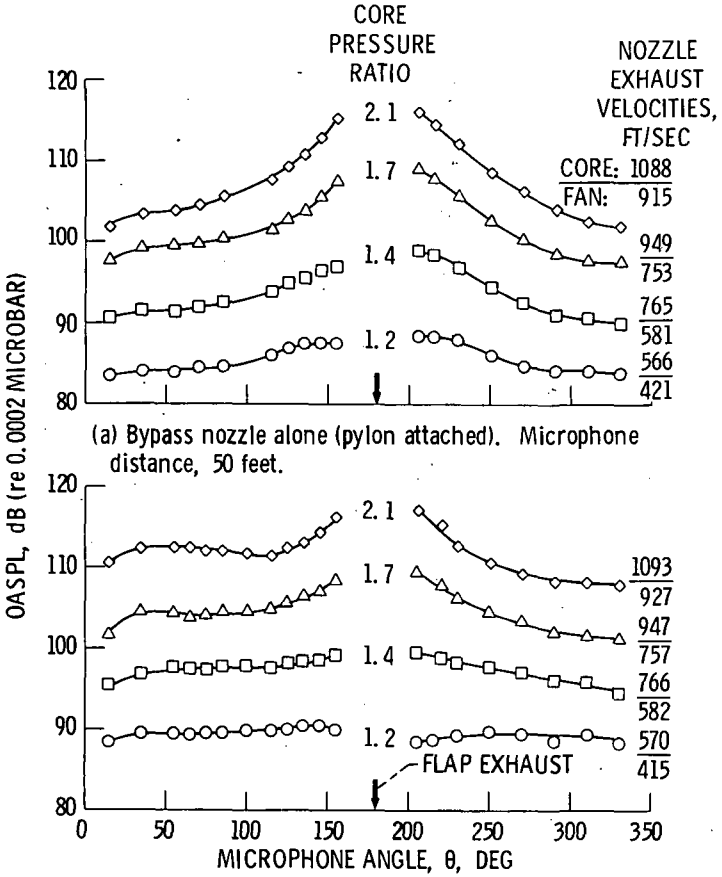

(a) Bypass nozzle alone (pylon attached). Microphone distance, 50 feet.

(b) Flap angle, 0^{o} (retracted); microphone distance, 50 feet.

Figure 9. - Effect of bypass nozzle exhaust velocities on overall sound pressure level.

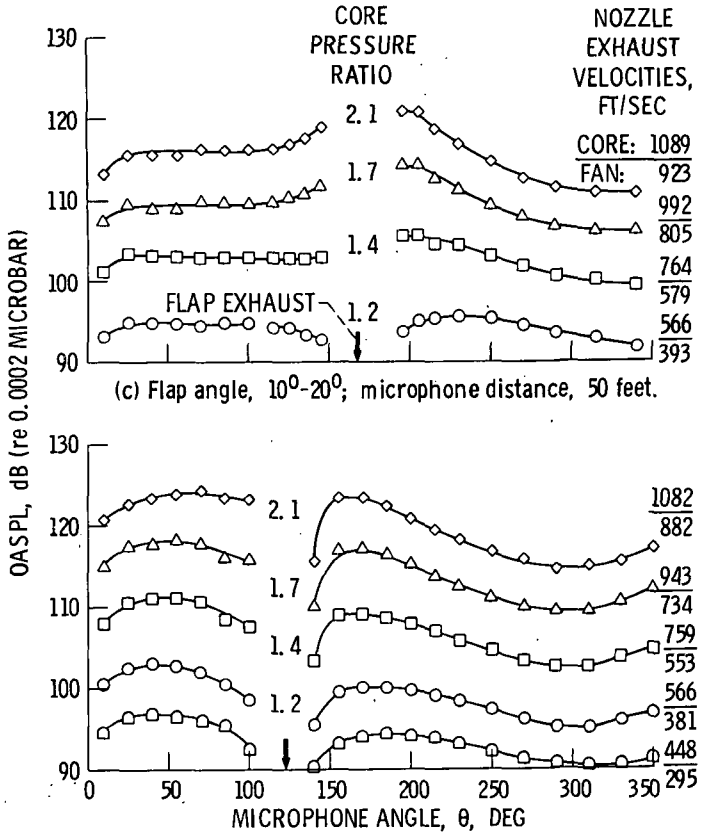

(c) Flap angle, 10^{o}-20^{o}; microphone distance, 50 feet.

(d) Flap angle, 30^{o}-60^{o}; microphone distance, 50 feet.

Figure 9. - Concluded.

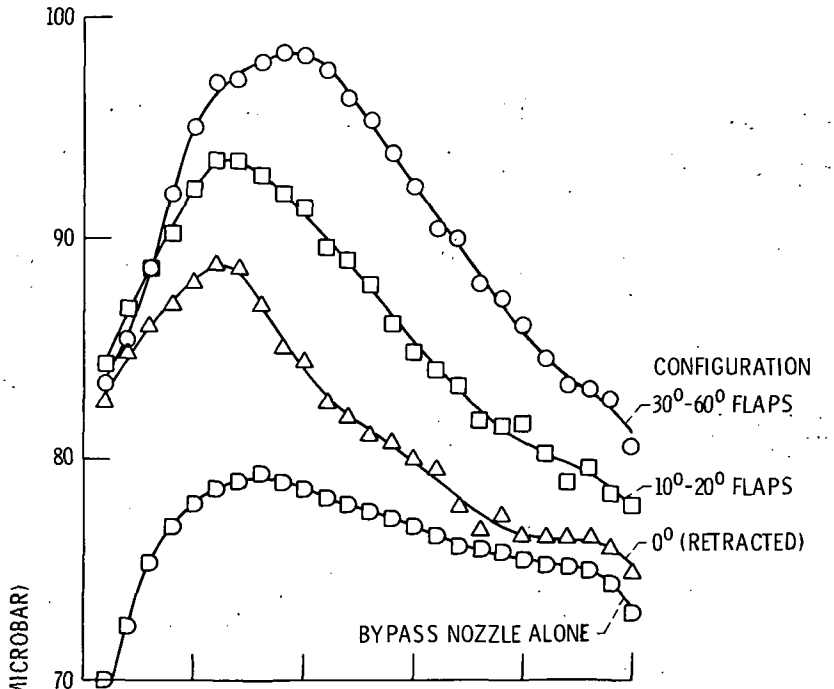

(a) Core nozzle pressure ratio, 1.4. Core velocity, 765 ft/sec; fan velocity, 581 ft/sec.

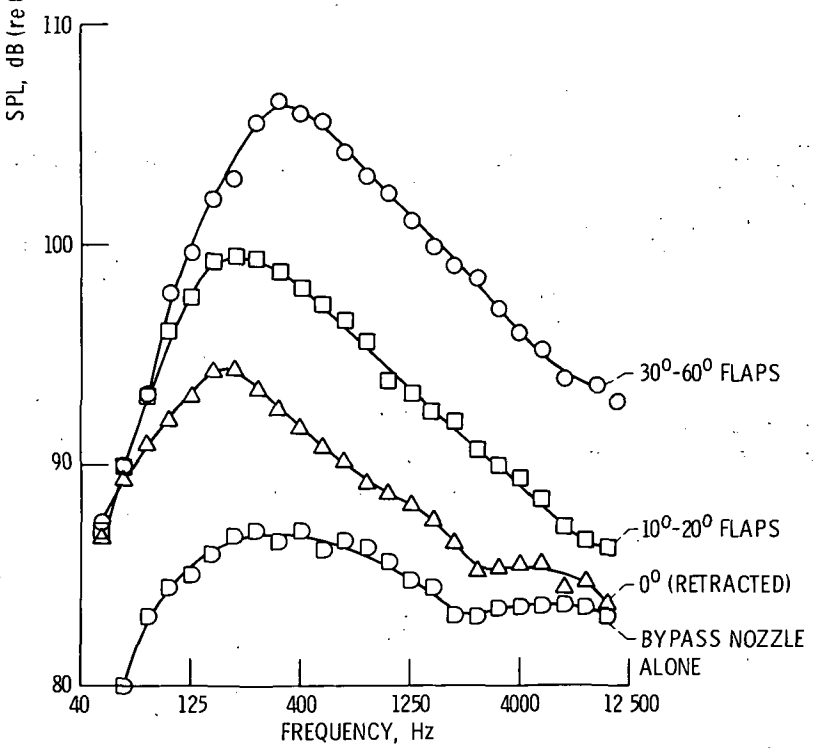

(b) Core nozzle pressure ratio, 1.7. Core velocity, 945 ft/sec; fan velocity, 754 ft/sec.

Figure 10. - Blown flap 1/3-octave spectra for the four test configurations. Microphone angle, 85°. Distance, 50 feet.

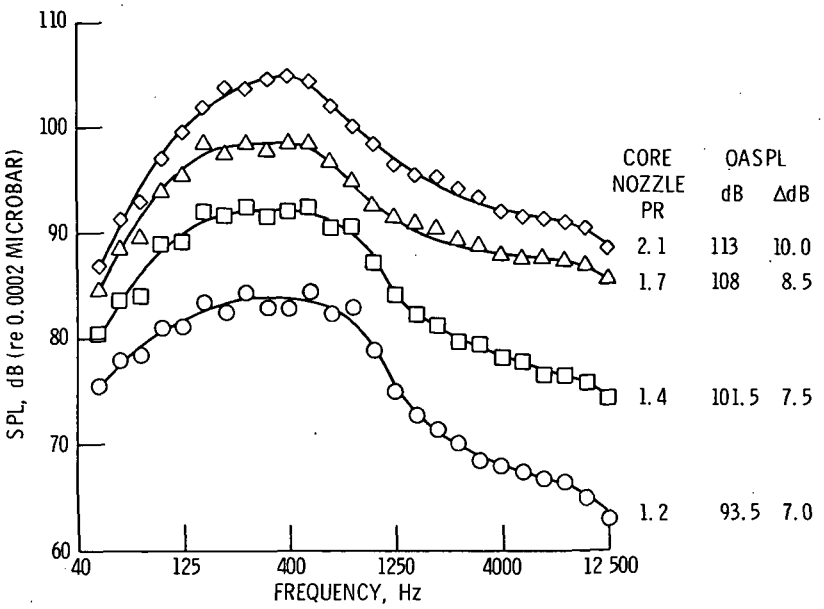

Figure 11. - Sideline 1/3-octave spectra measured with overhead microphone. Distance, 50 feet. Flap setting, 30^{0}-60^{0}.

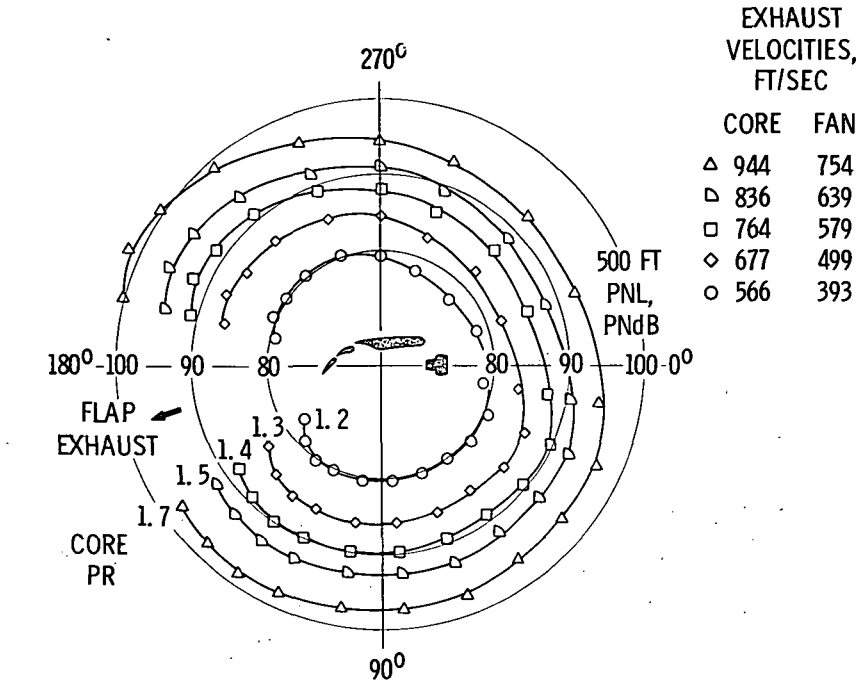

(a) Flap angle, 10°-20°.

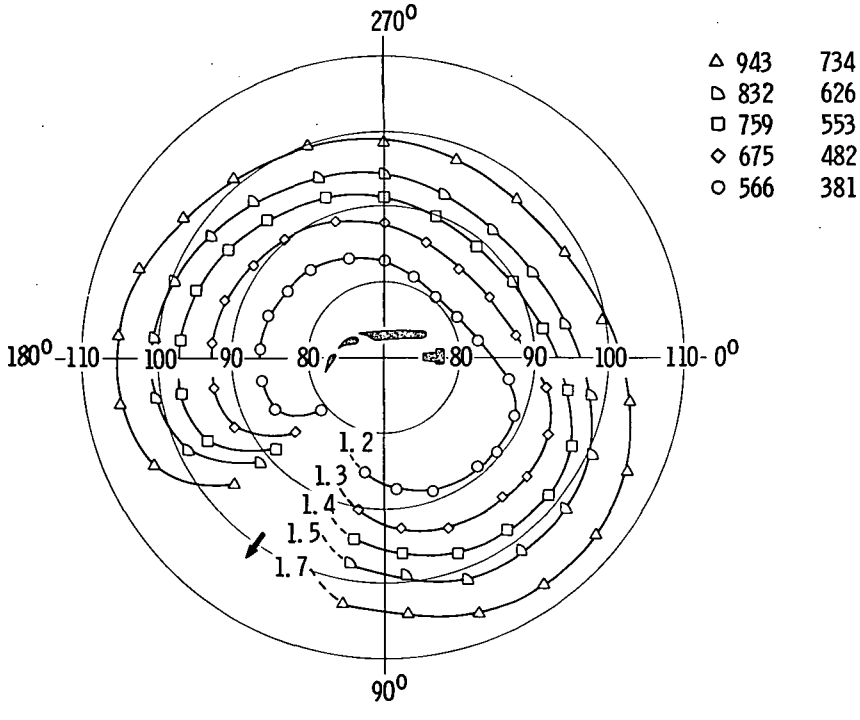

(b) Flap angle, 30°-60°.

Figure 12. - Perceived noise level radiation pattern for 1/2-scale EBF model at 500 feet.

E-6737

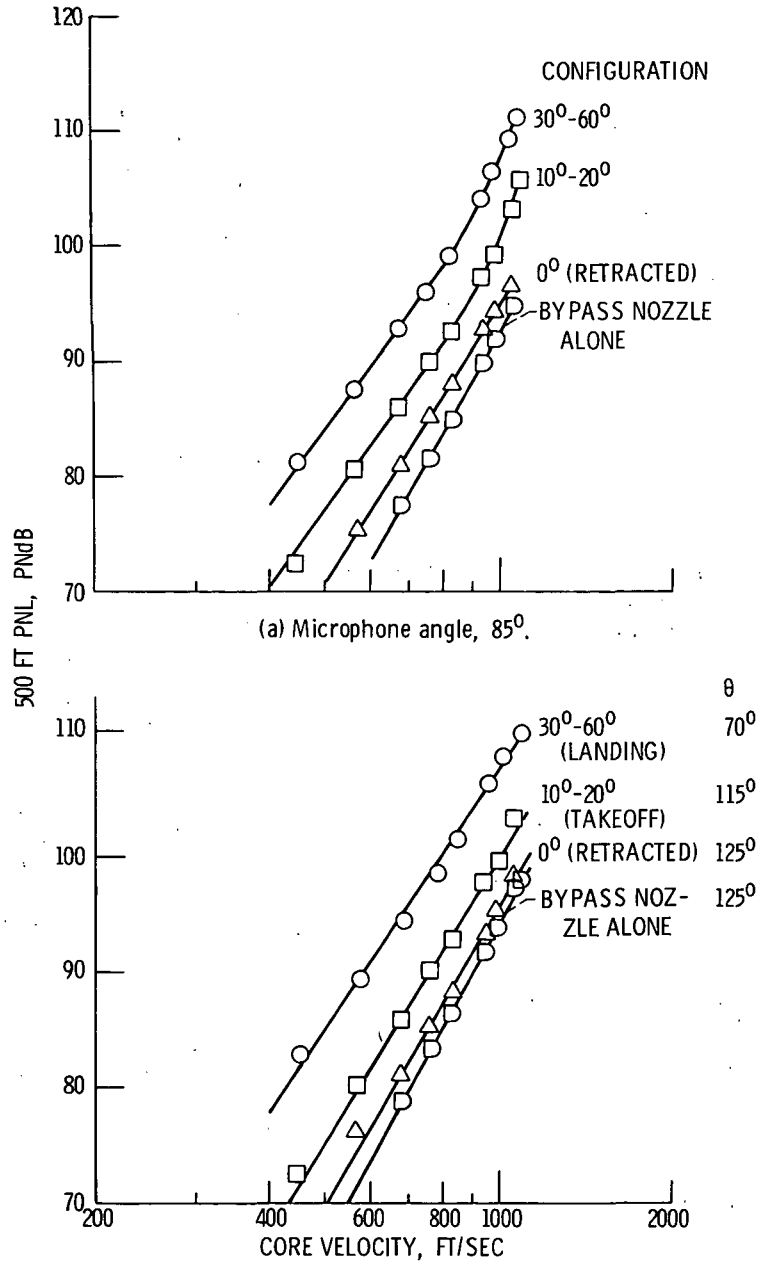

(b) At microphone angle, θ, producing flyover maximum.

Figure 13. - Variation of perceived noise level at 500 feet from 1/2-scale EBF model with core exhaust velocity.

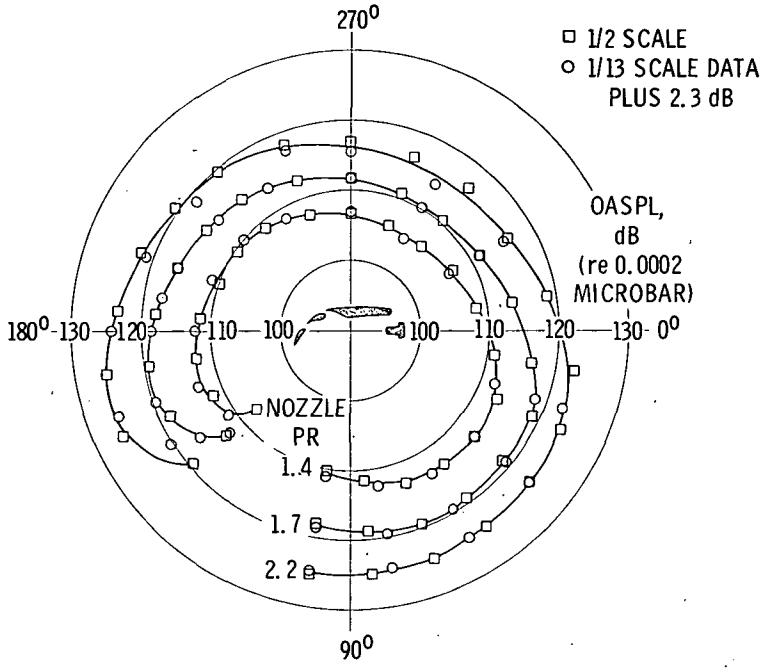

Figure 14. - Comparison of large and small model radiation patterns. Small model data scaled up to 1/2-scale size. Flap angle, 30°-60°. Distance, 50 feet.

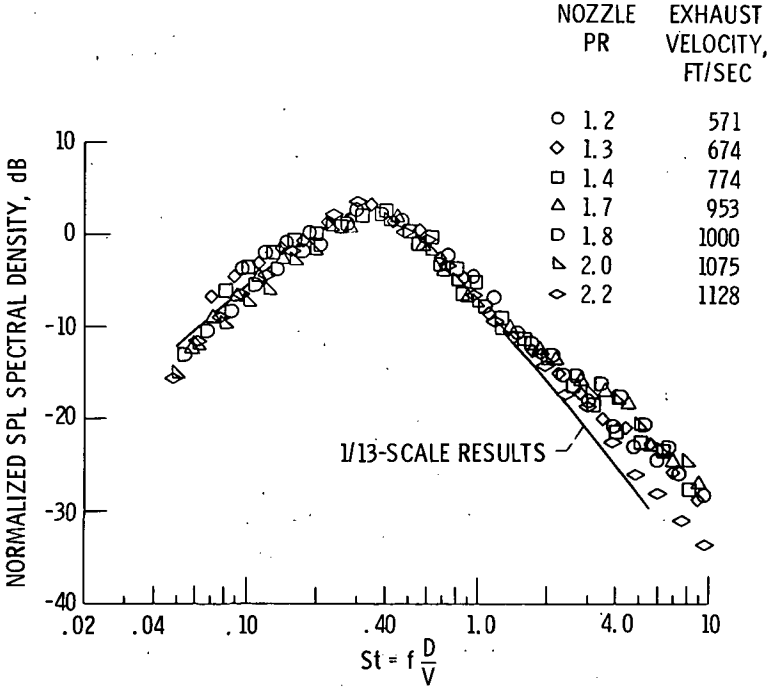

Figure 15. - Strouhal correlation of 1/2-scale model data. Curve shown for comparison was obtained from 1/13-scale model correlation. Flap setting, 30°-60°; microphone angle, 85°.

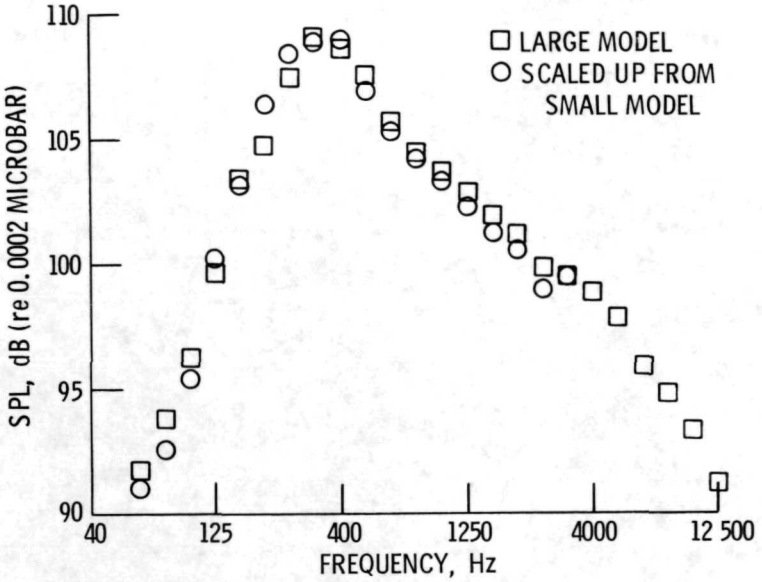

Figure 16. - Comparison of 1/2-scale data with spectrum obtained by scaling up 1/13-scale data. Flap angle, 30^0-60^0. Nozzle pressure ratio, 1.7. Microphone distance, 50 feet. Microphone angle, 85^0.

EBF STOL AIRCRAFT

70,000 LB GROSS WEIGHT

4 - 10,000 LB_f ENGINES

BYPASS RATIO, 6. AREA RATIO, 3. $V_{FAN}/V_{CORE} = 0.78$.

FLIGHT CONDITIONS

	TAKEOFF	LANDING
FLAP SETTING, DEG	10-20	30-60
ENGINE EXHAUST VELOCITIES, FT/SEC		
FAN	850	680
CORE	1090	870
BLOWN FLAP NOISE, PNdB		
FLYOVER	116	113
SIDELINE	111	105

Figure 17. - Perceived noise level estimates for full scale STOL aircraft at 500 feet based on 1/2-scale results.

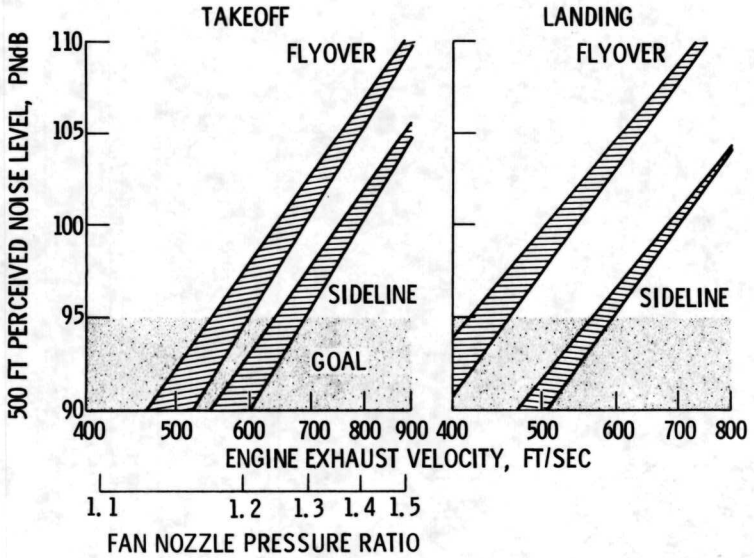

Figure 18. - Effect of engine exhaust velocity on perceived noise level at 500 feet for an externally blown flap system. Aircraft gross weight, 70 000 lbs; total thrust (4 engines), 40 000 lb_f.

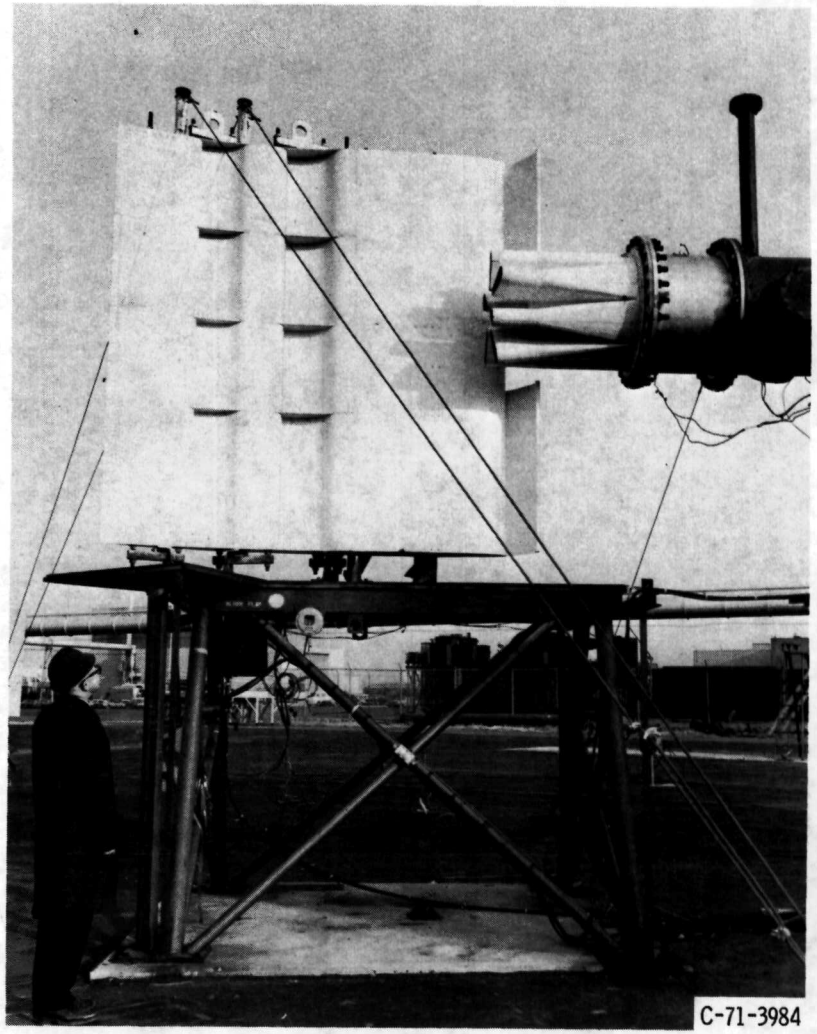

Figure 19. - Externally-blown-flap model with research mixer nozzle.